



Nitrate preservation in snow at Dome A, East Antarctica from ice core concentration and isotope records

Su Jiang^a, Guitao Shi^{b,a,*}, Jihong Cole-Dai^c, Lei Geng^d, Dave G. Ferris^e, Chunlei An^a, Yuansheng Li^a

^a Polar Research Institute of China, Shanghai, 200136, China

^b Key Laboratory of Geographic Information Science, School of Geographic Sciences and Institute of Eco-Chongming, East China Normal University, Shanghai, 200241, China

^c Department of Chemistry and Biochemistry, South Dakota State University, Avera Health and Science Center, Box 2202, Brookings, SD, 57007, United States

^d Anhui Province Key Laboratory of Polar Environment and Global Change, School of Earth and Space Sciences, University of Science and Technology of China, Hefei, Anhui, 230026, China

^e Department of Earth Sciences, Dartmouth College, Hanover, NH, 03755, United States



ARTICLE INFO

Keywords:

Nitrate
Preservation
Isotopes
Ice core
Dome A

ABSTRACT

A shallow ice core from Dome A (DA2005 ice core), East Antarctica is used to investigate the preservation and variation of nitrate (NO_3^-) at a location with extremely low snow accumulation rate. The average NO_3^- concentration of $11.8 \pm 3.0 \mu\text{g kg}^{-1}$ in the last 2840 years covered by the top 100.42 m is the lowest in all Antarctic ice cores for this specific temporal frame. Isotopic composition of NO_3^- indicates that NO_3^- in the DA2005 core has experienced strong post-depositional processing most likely driven by photolytic chemistry, which results in the extremely low NO_3^- concentration. NO_3^- remaining at depth far below the surface is mainly cycled and produced locally. A decrease in NO_3^- concentration from AD 1250 to 1900 and a sustained NO_3^- dip in AD 1500–1900 below the long-term mean concentration may be linked with changes in primary NO_x sources. In the DA2005 core, significant NO_3^- displacement is observed in layers containing volcanic sulphate; the degree of displacement is largely influenced by the volcanic signal magnitude, i.e., large volcanic signals lead to significant displacement, while small signals result in negligible displacement. In addition, it is found that snow accumulation rate could influence NO_3^- displacement by comparing DA2005 core and other Antarctic ice core records.

1. Introduction

Nitrogen oxides ($\text{NO}_x = \text{NO} + \text{NO}_2$) play an important role in tropospheric chemistry and the oxidation capacity of the atmosphere. The cycle between NO and NO_2 acts as the primary ozone (O_3) source in the troposphere, and the removal of NO_x through oxidation to nitrate (NO_3^-) consumes O_3 and OH radicals (Wolff et al., 2002; Alexander et al., 2009). NO_3^- in polar snow is considered a final sink for atmospheric NO_x ; and NO_3^- records from polar ice cores are expected to provide information about past variations in atmospheric NO_x sources and oxidation capacity (Dibb et al., 1998; Hastings et al., 2005). To date, a number of NO_3^- records from Antarctic ice cores have been reported (Legrand and Kirchner, 1990; Watanabe et al., 1999; Röthlisberger et al., 2000; Wolff et al., 2010; Laluraj et al., 2011). However, interpretation of ice core NO_3^- records in terms of NO_x

source variations has been shown to be difficult, for processes driving the variability of NO_3^- in snow have turned out to be extremely complicated (Legrand et al., 1999; Wolff et al., 2008). In particular, it has been recognized that NO_3^- in near surface snow can be lost or re-emitted into the atmosphere as NO_x , which may be subsequently oxidized and deposits as NO_3^- with fresh snow (Frey et al., 2009; Erbland et al., 2013; Shi et al., 2018a). It has also been found that these post-depositional processes (NO_3^- air-snow exchange, or the NO_x cycling) strongly influence the NO_3^- concentration preserved in snow (Röthlisberger et al., 2000; Blunier et al., 2005; Grannas et al., 2007). The degree of post-depositional processing and, consequently, the NO_3^- concentration ultimately preserved in depth are affected by glaciological factors such as snow accumulation rate and climatological factors including solar radiation and local temperature (Röthlisberger et al., 2000, 2002; Warren et al., 2006; Zafko et al., 2013). To properly

* Corresponding author. Key Laboratory of Geographic Information Science, School of Geographic Sciences and Institute of Eco-Chongming, East China Normal University, Shanghai, 200241, China.

E-mail address: gt_shi@163.com (G. Shi).

<https://doi.org/10.1016/j.atmosenv.2019.06.031>

Received 5 December 2018; Received in revised form 13 June 2019; Accepted 16 June 2019

Available online 18 June 2019

1352-2310/© 2019 Elsevier Ltd. All rights reserved.

interpret ice core NO_3^- records in terms of variations in NO_x source and atmospheric oxidation capacity, the influence of these factors must be understood and their effect quantified.

Nitrogen isotopic composition of snow NO_3^- may preserve signatures of different NO_x sources (Xiao and Liu, 2002; Hastings et al., 2003; Elliott et al., 2007). During NO_x cycling and its conversion into NO_3^- in the atmosphere, oxygen atoms from oxidants (e.g., OH and O_3 , which possess distinct oxygen isotopic signatures) are incorporated into NO_3^- . Accordingly, oxygen isotopes of NO_3^- can provide valuable information regarding the abundances of the oxidants (i.e., oxidation capacity of the atmosphere) and the relative contribution to NO_3^- formation by various reaction pathways (Alexander et al., 2009; Michalski et al., 2012). Thus, the measurement of isotopic composition of NO_3^- can contribute to interpreting ice core NO_3^- records (e.g. Sofen et al., 2014).

The Little Ice Age (LIA), a relatively cold period from approximately the beginning of the fifteenth century to the middle or end of the nineteenth century, is the most prominent multi-century scale climate feature in the last millennium. NO_3^- concentrations have been found to be low during AD 1450–1850 at DT263, a site located near Dome A in East Antarctica with the average accumulation rate of $33 \text{ kg m}^{-2} \text{ a}^{-1}$ during this period (Li et al., 2009). The decrease of NO_3^- concentration during AD 1500–1900 is also seen in a composite ice core record from Dronning Maud Land (DML) in Antarctica (Pasteris et al., 2014). However, in an ice core drilled at Dome C (average accumulation rate of $27 \text{ kg m}^{-2} \text{ a}^{-1}$), East Antarctica and an ice core from WAIS Divide (present-day annual accumulation rate of $220 \text{ kg m}^{-2} \text{ a}^{-1}$) in West Antarctica, NO_3^- concentration apparently did not decrease in the time period of 1400s–1800s (Röthlisberger et al., 2000; Sofen et al., 2014). It appears that the LIA effect on NO_3^- in snow and, indeed, the occurrence of LIA across Antarctica, remains insufficiently documented and the reasons for the effect are poorly understood, and ice core NO_3^- records from additional locations are needed to document the spatial variation of LIA and to assess the climate impact on snow NO_3^- .

Below the near surface zone, which is typically in the depth interval of surface to 0.6 m, where air-snow exchange plays an important role, NO_3^- concentration is expected to be locked in or preserved with depth. However, observations suggest that NO_3^- concentration may be altered by the presence of certain chemical impurities in the snow strata (Legrand et al., 1999; Röthlisberger et al., 2000). For example, instances of displacement of NO_3^- by high concentrations of sulphuric acid (H_2SO_4) from volcanic eruptions have been found in Antarctic and Greenland ice cores (Röthlisberger et al., 2000, 2002). However, the proposed mechanisms for this effect have not been vigorously tested, because of a lack of high-resolution ice core records.

Dome Argus (Dome A), located along the main glaciological dividing line of the East Antarctic Plateau, has the highest elevation in East Antarctica (Fig. 1). The snow accumulation rate of $23.2 \text{ kg m}^{-2} \text{ a}^{-1}$ at Dome A (Jiang et al., 2012) is among the lowest in Antarctica. A study by Shi et al. (2018a) suggests that the low snow accumulation rate at Dome A would lead to significant post-depositional loss of NO_3^- from near surface snow. In this study, we report the measurements of concentration and stable isotopic composition of NO_3^- in a shallow Dome A ice core covering the last 2840 years. Our main objectives are (1) to determine the degree of post-depositional processing of snow NO_3^- and the extent of NO_3^- preservation in snow below the air-snow exchange zone, (2) to discern NO_3^- variation trend(s) in the last 2840 years, especially during LIA, and (3) to investigate the effect of volcanic events of various magnitude on NO_3^- displacement. The results of this study provide information on understanding of NO_3^- loss/preservation mechanisms and quantitative aspects of post-depositional processes in ice cores recovered from low accumulation sites, which can contribute to interpreting ice core NO_3^- records from low accumulation sites with confidence in terms of variations of atmospheric NO_x loading and oxidation capacity over time.

1.1. Ice-core sampling, analysis and dating

During the 21st Chinese Antarctic Research Expedition (CHINARE) in the 2004/2005 austral summer, a shallow ice core (DA 2005) was recovered at a site approximately 300 m from the summit of Dome A (80.37°S , 77.37°E , 4092.5 m above sea level) (Fig. 1). The DA2005 core was drilled with an electromechanical drill, and started at ~ 0.4 m from the 2005 snow surface and reached 109.91 m depth. The bulk density of each of the 80 cm long snow/ice cylinders was measured in the field. The cylinders were then wrapped in clean plastic sheets and shipped frozen to Polar Research Institute of China in Shanghai, China.

One-half (cross section) of the DA2005 core was transported to the Ice Core and Environmental Chemistry Laboratory (ICECL) at South Dakota State University, USA. The top 100.42 m was analyzed for major chemical impurities and NO_3^- isotopes. One-quarter (cross section) of the core was analyzed for the concentrations of major chemical impurities (Na^+ , NH_4^+ , K^+ , Mg^{2+} , Ca^{2+} , Cl^- , NO_3^- , and SO_4^{2-}) by the technique of continuous flow analysis coupled with ion chromatography (CFA-IC) at ICECL, with an average depth resolution of 13 mm per sample, as described in Jiang et al. (2012).

A total of 22 samples were obtained from the other quarter of the core in the depth interval of 8.98–100.42 m for NO_3^- isotopes analysis. In order to obtain sufficient amount of NO_3^- (about 500 nmol) for replicate measurements for isotope measurement, each sample covered a depth interval from 3 m to 7 m. The samples were melted at room temperature and concentrated using the resin method as described by Frey et al. (2009), to 10 mL solutions and stored frozen until the next analysis. Measurements of N and O isotope ratios of NO_3^- in the DA2005 core were performed in the stable isotope laboratory at University of Washington using the bacterial denitrifier method (Kaiser et al., 2007). Details on the isotopic measurements are described in Geng et al. (2014). Briefly, the denitrifying bacteria (*Pseudomonas aureofaciens*) lacking the N_2O reductase enzyme was used to convert NO_3^- in samples to $\text{N}_2\text{O}(\text{g})$, which was thermally decomposed to N_2 and O_2 in a heated gold tube. The gases were then separated by gas chromatography, followed by the measurements at m/z 28 and 29 from N_2 , and m/z 32, 33 and 34 from O_2 on an isotope ratio mass spectrometer. The isotopic ratios are expressed as delta notation, $\delta^{15}\text{N}$, $\delta^{17}\text{O}$ and $\delta^{18}\text{O}$, where δ (‰) = $(R_{\text{sample}}/R_{\text{reference}} - 1) \times 1000$, with R_{sample} and $R_{\text{reference}}$ denoting the isotope ratios ($^{15}\text{N}/^{14}\text{N}$, $^{18}\text{O}/^{16}\text{O}$ and $^{17}\text{O}/^{16}\text{O}$) in sample and in reference, respectively. The references are air N_2 and Vienna Standard Mean Ocean Water (VSMOW) for N and O, respectively. The isotope ratios of N and O in samples were calibrated against international reference materials, IAEA-NO-3 and USGS34 for N, and USGS34 and USGS35 for O. The oxygen-17 excess ($\Delta^{17}\text{O}$) was then calculated by using the linear approximation $\Delta^{17}\text{O} \approx \delta^{17}\text{O} - 0.52 \times \delta^{18}\text{O}$. The uncertainty (1σ) of $\delta^{15}\text{N}$ measurement was 1.0‰ based on replicate measurements of the international materials, while the analytical uncertainty of $\Delta^{17}\text{O}$ and $\delta^{18}\text{O}$ was estimated to be 0.1‰ and 0.5‰, respectively. Due to lower NO_3^- mass than the minimum size required for analysis, no reliable isotope results were obtained from the bottom 4 samples in the depth range of 86.66–100.42 m covering the period from 840 BC to 352 BC.

Dating of the DA2005 core was based on calculating mean accumulation rate between Samalas (1257) and Agung (1963) which are the two well-documented volcanic stratigraphic markers (Delmas et al., 1992; Cole-Dai et al., 2000; Lavigne et al., 2013), and several other well-documented volcanic signals, such as Kuwae (1458), Krakatau (1883) and Taupo (186) (Zielinski et al., 1994; Cole-Dai et al., 1997, 2000; 2013), were used to measure dating uncertainty (Jiang et al., 2012). The result shows that the upper 100.42 m of the core covers the last 2840 years before present, i.e., from 840 BC to AD 1998, and dating uncertainty is less than 11 years (Jiang et al., 2012). NO_3^- isotope record in the depth range of 8.98–86.66 m covers the time period from 352 BC to AD 1838.

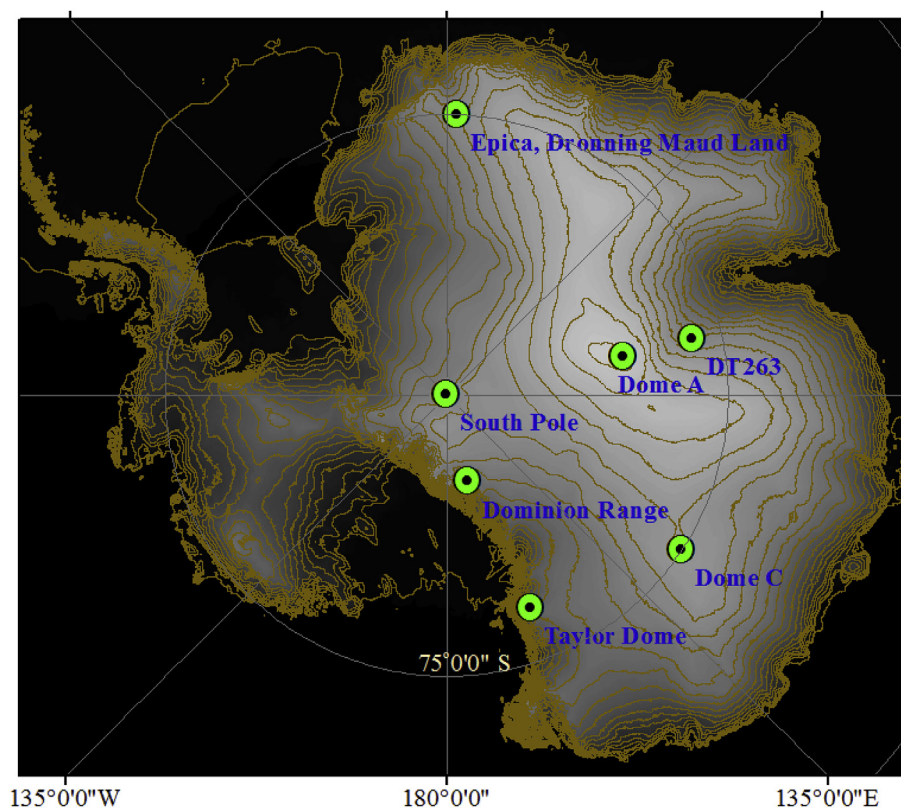


Fig. 1. Locations of ice core sites in Antarctica referred to the text.

2. Results and discussion

2.1. Nitrate preservation at Dome A

The DA2005 NO_3^- concentration profile is shown in Fig. 2a. Because no sample was collected from the top 0.4 m from the 2005 snow surface, a sharp decrease of NO_3^- with depth in the top meter, which is typical of NO_3^- profile at low accumulation sites (Röthlisberger et al., 2000; Traversi et al., 2009), is not observed in the DA2005 core. The NO_3^- concentration varies between 2.9 and 30.8 $\mu\text{g kg}^{-1}$. The average NO_3^- concentration of 11.8 $\mu\text{g kg}^{-1}$ at Dome A is the lowest among those (Table 1) reported for Antarctic ice cores covering several hundred years or longer. For example, the average NO_3^- concentration at South Pole is approximately 84 $\mu\text{g kg}^{-1}$ and about 14 $\mu\text{g kg}^{-1}$ at Dome C.

Snow accumulation rate is thought to be a key factor influencing NO_3^- concentration preserved in snow/ice. Since post-depositional loss of NO_3^- mainly occurs in the shallow snowpack ($\sim 0\text{--}0.6$ m; France et al., 2011; Zatko et al., 2013), NO_3^- deposited in the snow at locations with a low snow accumulation rate (such as Dome A) is not quickly buried by new snow and spends a long period of time near the surface when NO_3^- is gradually lost. Therefore, the extremely low NO_3^- concentration in the DA2005 core suggests that an unusually small fraction of NO_3^- in fresh snow is preserved in deeper snow at Dome A, which appears to be the result of a high degree of post-depositional loss.

It has been established that an important mechanism of NO_3^- loss is the photolysis of NO_3^- leading to formation and emission of NO_x from the snowpack. Moreover, Frey et al. (2009) have shown that photolytic loss can significantly enrich $\delta^{15}\text{N}$ of snow NO_3^- . $\delta^{15}\text{N}$ of NO_3^- in the DA2005 core varies between 235 and 279‰ (Fig. 2b), with an average of 265‰. The relatively high $\delta^{15}\text{N}$ of NO_3^- in the DA2005 core is consistent with the $\delta^{15}\text{N}$ values (111‰ (upper snow) and 461‰ (deeper snow), with a mean of 335‰) in a Dome A snowpit reported by

Shi et al. (2015). The larger range of $\delta^{15}\text{N}$ in the snowpit than that in the DA2005 core is likely associated with the smoothing effect due to large sample size (i.e., the time resolution of $\delta^{15}\text{N}$ of NO_3^- in the DA2005 core is rather low, $\sim 100\text{--}200$ years per sample).

The $\delta^{15}\text{N}$ values in the DA2005 core (> 200 ‰) are much higher than that of NO_x of most sources, e.g., soil emissions (Yu and Elliott, 2017; and references therein), lightning (Hoering, 1957), fossil fuel combustion (Miller et al., 2017), and biomass burning (Fibiger and Hastings, 2016). This suggests that they are likely the result of high degree of post-depositional processing ($\text{NO}_3^-/\text{NO}_x$ cycling driven by photolytic loss and re-deposition), rather than of high $\delta^{15}\text{N}$ of primary NO_x sources. In addition to photolysis, volatilization of HNO_3 is another mechanism for NO_3^- loss in Antarctic snow, accompanied by fractionation of NO_3^- isotopes (Frey et al., 2009; Berhanu et al., 2015). The HNO_3 volatilization, however, is thought to be rather minor at temperatures below -30°C (Frey et al., 2009; Berhanu et al., 2015). At Dome A, where annual mean temperature is below -50°C (Ma et al., 2010), post-depositional loss of snow NO_3^- is mainly driven by photolysis near the surface. Consequently, both the extremely low preserved NO_3^- concentration and high $\delta^{15}\text{N}$ of NO_3^- in the DA2005 core lead to the likely conclusion that photolytic loss is the main loss mechanism, which is enhanced by the slow burial of fresh snow owing to the very low accumulation rate at Dome A. Previous reports suggest that the trend of low NO_3^- concentration and significant enrichment of ^{15}N at deeper depths at low accumulation sites could be predicted with the assumption that NO_3^- variation is driven by photolytic loss (Erbland et al., 2013). However, no relationship was found between concentrations and $\delta^{15}\text{N}$ of NO_3^- in the DA2005 core (Fig. S1), suggesting that NO_3^- concentration variations are also influenced by other factors including NO_x source strength. Thus, much more information exists in the observations than can be explained by the simple assumption that photolytic loss is the only factor driving the variation of NO_3^- .

In coastal regions of Antarctica and Greenland, where snow

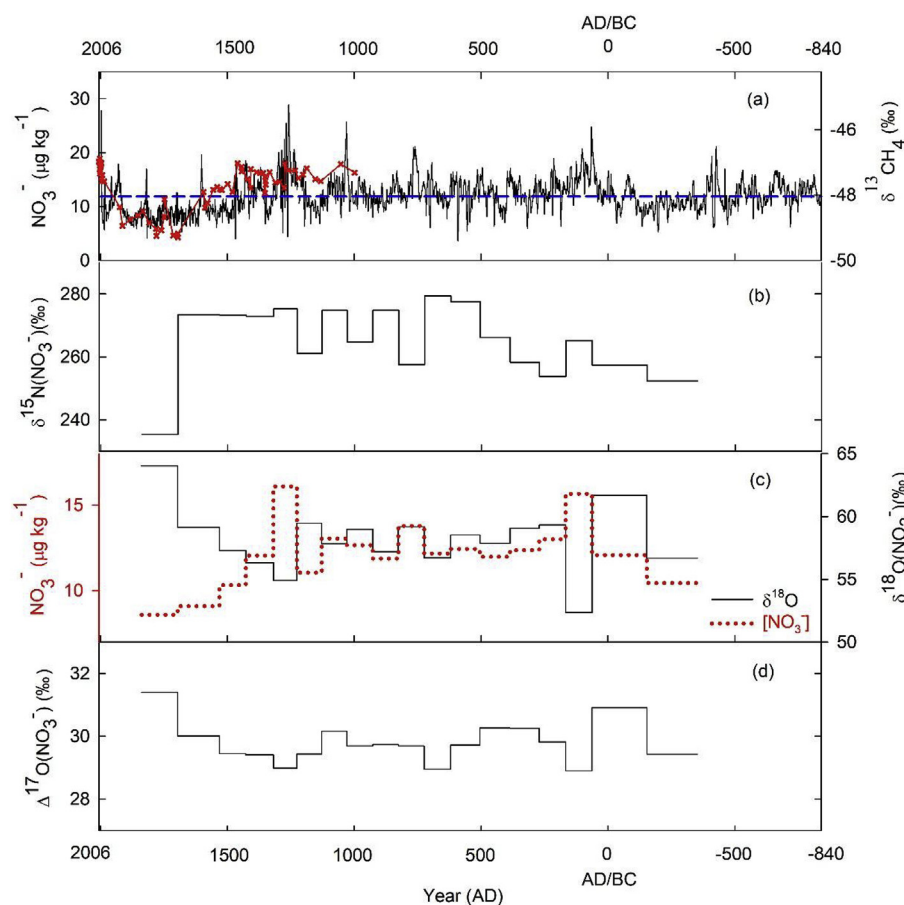


Fig. 2. Annual mean concentration (a) and isotopes of NO_3^- (b, c and d) in the DA2005 core. In panel (a), the dashed horizontal blue line represents the mean NO_3^- concentration over the last 2840 years, and the red dots represents the methane carbon isotopes ($\delta^{13}\text{C}_{\text{CH}_4}$) from WAIS Divide over the last 1000 years. In panel (c), the dotted red line shows NO_3^- average concentrations in the same time resolution to that of $\delta^{18}\text{O}(\text{NO}_3^-)$.

accumulation is generally higher than $100 \text{ kg m}^{-2} \text{ a}^{-1}$, relatively low NO_3^- concentrations are generally associated with high snow accumulation rate (Röthlisberger et al., 2002; Shi et al., 2018b), rather than with low accumulation. This may indicate that the dilution effect by snowfall is more significant than reduced loss by photolysis. Indeed, Weller et al. (2004) proposed that post-depositional loss of NO_3^- becomes insignificant at locations with accumulation rate above $100 \text{ kg m}^{-2} \text{ a}^{-1}$. For instance, in coastal Antarctica, the initially deposited NO_3^- is thought to be largely preserved with minimal snowpack reprocessing (Shi et al., 2015, 2018b). Similarly, investigations at Summit, Greenland (with the accumulation rate of $\sim 200 \text{ kg m}^{-2} \text{ a}^{-1}$) showed that the post-depositional loss of NO_3^- is rather minor and the variations of the isotopic signal appears to be largely preserved (Hastings et al., 2004; Fibiger et al., 2013). While the archived fraction of NO_3^- at low snow accumulation sites is largely dependent on the reprocessing in snowpack, ice core NO_3^- concentrations in high snow accumulation regions likely reflect directly variations in atmospheric NO_x burden, which is also supported by the modelling work results (Erbland et al., 2015; Zatzko et al., 2016).

2.2. Nitrate cycling suggested by oxygen isotopes

$\delta^{18}\text{O}$ and $\Delta^{17}\text{O}$ of NO_3^- in the DA2005 core fall in the ranges of 52.4–64.0‰ (mean = 58.1‰) and 28.9–31.4‰ (mean = 29.8‰), respectively (Fig. 2c and d), with $\delta^{18}\text{O}$ lower than that reported for NO_3^- in West Antarctic snow and ice and comparable $\Delta^{17}\text{O}$ (Sofen et al., 2014). The two data profiles both exhibit steady increase during AD 1250–1838, with highest values in the most recent sample (i.e., 64.0‰ and 31.4‰ for $\delta^{18}\text{O}$ and $\Delta^{17}\text{O}$, respectively). In the last 2200 years, $\delta^{18}\text{O}$ and $\Delta^{17}\text{O}$ vary in-phase, and a significant linear relationship was found ($R^2 = 0.73$, $p < 0.01$; Fig. 3a). The variation patterns of oxygen isotopes are generally opposite to that of $\delta^{15}\text{N}$ (Fig. 3b and c). The relationships among NO_3^- isotopes in the DA2005 core are consistent with those in inland Antarctic surface snow (Shi et al., 2018a).

$\Delta^{17}\text{O}$ represents the mass-independent relationship between $\delta^{17}\text{O}$ and $\delta^{18}\text{O}$ (McCabe et al., 2007). In typical mass-dependent fractionation processes, the isotope ratios of oxygen always follow an approximately linear relationship, i.e., $\delta^{17}\text{O} \approx 0.52 \times \delta^{18}\text{O}$, and deviation from the linear relationship is called mass-independent fractionation (MIF). As a mass-dependent process, it is expected that photolytic loss

Table 1

Nitrate concentration and accumulation rates for different Antarctic sites.

Ice core drilling sites	Nitrate concentration, $\mu\text{g kg}^{-1}$	Accumulation rate, $\text{kg m}^{-2} \text{ a}^{-1}$	Period covered	References
Dome A (80.37°S, 77.37°E)	11.8	23	2840 years BP (present = 1998 AD)	this work
Dome C (75.01°S, 123.40°E)	13.7	27	3170 years BP (present = 1950 AD)	Röthlisberger et al. (2000)
Taylor Dome (77.78°S, 158.72°E)	52.2	65	3000 years BP (present = 1950 AD)	Mayewski et al. (1996)
DT263 (76.54°S, 77.03°E)	20.5	33	1451–1800 AD	Li et al. (2009)
Dronning Maud Land (75.00°S, 2.00°E)	54.4	77	1865–1991 AD	Isaksson et al. (1996)
Dominion Range (85.25°S, 166.17°E)	34.3	35	3000 years BP (present = 1950 AD)	Mayewski et al. (1995)
South Pole (89.96°S, 17.67°W)	84.3	75	176–2004 AD	Ferris et al. (2011)

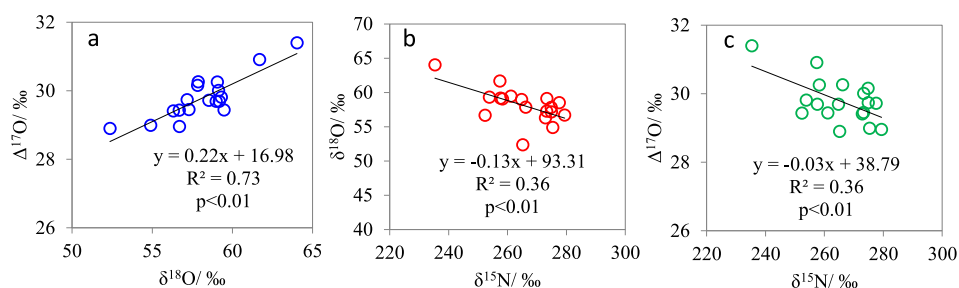


Fig. 3. Relationships among isotopic composition of NO_3^- ($\delta^{15}\text{N}$, $\delta^{18}\text{O}$ and $\Delta^{17}\text{O}$) in the DA2005 core.

of NO_3^- alone will not change $\Delta^{17}\text{O}$ in the preserved part of snow NO_3^- (McCabe et al., 2005), but will increase $\delta^{18}\text{O}$ of NO_3^- remaining in the snowpack (i.e., a negative fractionation constant for ^{18}O , similar to that of ^{15}N ; Frey et al., 2009). However, high $\delta^{15}\text{N}$ values generally correspond to low oxygen isotopic ratios (Figs. 2 and 3). During NO_3^- photolysis in the snowpack, some of the photoproducts (e.g., NO_2^-) remain in the condensed phase and undergo re-oxidation reactions to yield NO_3^- . In this case, oxygen atoms of OH and/or H_2O , with extremely low $\delta^{18}\text{O}$ ($< -50\text{‰}$; Xiao et al., 2008; Shi et al., 2018a) and $\Delta^{17}\text{O} \approx 0$, will be incorporated into the re-formed NO_3^- . Since the primary oxygen isotopic ratio of NO_3^- produced in the atmosphere is positive, resulting from the capture of the signature of O_3 (Vicars and Savarino, 2014), the values of $\delta^{18}\text{O}$ and $\Delta^{17}\text{O}$ in re-formed NO_3^- will be lowered. This mechanism is supported by experimental and simulation works (McCabe et al., 2005; Jacobi and Hilker, 2007) and has also been used to explain the observations on East Antarctic plateaus (Erland et al., 2013; Shi et al., 2018a). At the same time, some of the photoproducts (e.g., NO_2) will be released to the interstitial air and subsequently escape to the overlying atmosphere due to wind pumping. These products can also be re-oxidized to NO_3^- by the local oxidants (i.e., OH). The re-formed NO_3^- will re-enter the snowpack by precipitation, or be transported away. The linear relationship between oxygen isotopes of NO_3^- (Fig. 3a) further suggests the archived fraction in DA2005 is dominated by cycled NO_3^- , possibly reproduced in both condensed phase and gas phase.

2.3. Temporal variation of nitrate concentration in the DA2005 core

The most striking long-lasting feature in the 2840 year DA2005 NO_3^- record appears to be the reduced NO_3^- concentration during the period from approximately AD 1500–1900 (Fig. 2a). NO_3^- mean concentration ($8.8 \mu\text{g kg}^{-1}$) during this period is markedly lower than that prior to 1500 ($12.6 \mu\text{g kg}^{-1}$) and after 1900 ($10.9 \mu\text{g kg}^{-1}$, Table 2). As described in section 3.1, low NO_3^- concentration in Antarctic ice is generally related to low snow accumulation rate, thus the low NO_3^- concentration during 1500–1900 possibly suggests decreased snow accumulation rate in this period. Li et al. (2009) found that, at DT263, accumulation rate as well as NO_3^- concentration during this period were significantly reduced compared with other time periods covered by the DT263 core (AD 1207–1996). Long term variations in Antarctic snow accumulation rates appear to be directly related to and controlled

by climate change, with low snow accumulation in general during cold time periods (EPICA Community Members, 2004; Jouzel et al., 2007). For example, the reduced accumulation and NO_3^- concentration at DT263 during the period of 1450–1850 were interpreted by Li et al. (2009) as evidence of a LIA-type neoglaciation in this region of Antarctica. Using the DA2005 volcanic record by Jiang et al. (2012), we calculated the average accumulation rates during specific time periods based on the length of time between two volcanic eruptions and the depth interval between the two volcanic markers. Kuwae (1458) and Krakatau (1883), with their respective appearance time closest to the beginning and end of the AD 1500–1900 period in DA 2005, are used to calculate the average accumulation rate in AD 1458–1883. The signals of Taupo (186), Samalas (1257) and Agung (1963) are selected to calculate average accumulation rates prior to and after the period of AD 1458–1883. As seen in Table 2, the average accumulation rate in the period AD 1458–1883 is similar to those in AD1257–1457, AD 186–1256 and AD 1884–1963. Therefore, it appears that reduced accumulation is not responsible for the decreased NO_3^- concentration during 1500–1900 in the Dome A region.

A decrease of NO_3^- concentration during this time period was also seen in an ice core drilled at DML. Similar to that at Dome A, no sustained reduction in snow accumulation during AD 1500–1900 was observed in the DML region (Pasteris et al., 2014). Pasteris et al. (2014) found a close relationship ($r = 0.63$, $p < 0.0001$) between $\delta^{13}\text{C}$ of methane in the WAIS Divide ice core (Mischler et al., 2009) and NO_3^- in DML, and concluded that the NO_3^- decrease at DML was associated with the decreased atmospheric NO_x emitted by biomass burning. NO_3^- concentrations in the DA2005 core and $\delta^{13}\text{CH}_4$ data from WAIS Divide (Mischler et al., 2009) also show a high degree of similarity over the last 1000 years ($r = 0.52$, $p < 0.0001$ ($n = 53$); data pairs with the same time period) (Fig. 2a). This seems to suggest that the low NO_3^- concentration during this time period at Dome A is the result of reduced NO_x emission. However, snow accumulation rate is much lower at Dome A than in DML, and, as discussed earlier, NO_x cycling driven by photolysis strongly influences NO_3^- level preserved in the DA2005 core. The temporal variation of DA2005 NO_3^- concentration can also be influenced by the variability of photolysis. The isotope data here may provide clues to the extent of photolysis and/or the changes of NO_x sources during this period.

There is a steady decrease of NO_3^- concentration from AD 1250 to 1900 (Fig. 2a), while the oxygen isotopes exhibit the reverse pattern

Table 2

Average accumulation rates and NO_3^- mean concentrations during specific time periods in the DA2005 record.

Time period	Average Accumulation, $\text{kg m}^{-2} \text{a}^{-1}$	NO_3^- concentration, $\mu\text{g kg}^{-1}$	NO_3^- flux, $\mu\text{g m}^{-2} \text{a}^{-1}$	Deviation from AD 1458–1883, %		
				accumulation	concentration	flux
1884–1963	23.2	10.9	252.9	+1.3	+23.9	+25.5
1458–1883 (closest to the interval of 1500–1900)	22.9	8.8	201.5	0	0	0
1257–1457	23.7	12.8	303.4	+3.5	+45.5	+50.6
186–1256	23.4	12.6	294.8	+2.2	+43.2	+46.3

(Fig. 2c). If it is assumed that NO_x sources were stable and the decrease of NO_3^- was driven alone by increasing photolytic loss during this period, the lower NO_3^- concentrations (i.e., more photolytic loss of NO_3^-) would generally correspond to higher $\delta^{15}\text{N}$ of NO_3^- . However, $\delta^{15}\text{N}$ in DA2005 was relatively stable during AD 1226–1696 and decreased significantly in 1696–1838 (Fig. 2b), indicating no enhanced photolytic loss of NO_3^- during this period. No enhancement in photolytic loss is also supported by the opposite trends between NO_3^- concentration and oxygen isotopes during AD1250–1900. As discussed above, lower NO_3^- concentrations caused by enhanced photolytic loss would result in lower oxygen isotopic ratios due to cycling of NO_3^- with the assumption of invariant NO_x sources. However, the oxygen isotope trend appears to be in contradiction with the expected decrease in $\delta^{18}\text{O}$ and $\Delta^{17}\text{O}$. In this case, the data suggest that changes in NO_x sources are responsible for the low NO_3^- concentration during AD 1500–1900. Note that $\delta^{18}\text{O}$ increased by $\sim 10\text{‰}$ from AD 1250 to 1900 (Fig. 2c). The relatively constant snow accumulation rate (Table 2) and impurity (e.g., chemical ions) concentrations (Fig. S2) during this period tend to support no significant changes in photolysis of NO_3^- (Zatko et al., 2013). Because the NO_3^- oxygen isotope composition is influenced by that of the oxidants (O_3 and OH) in the troposphere, the combined data of NO_3^- concentration and isotope seem to indicate that the relative amounts of oxidants (O_3 and OH , responsible for separate formation pathways of NO_3^-) may have changed during AD 1250–1900.

2.4. Influence of volcanic sulphate on nitrate in the DA2005 core

Unusually high levels of sulphate or non-sea-salt sulphate ($\text{nssSO}_4^{2-} = \text{SO}_4^{2-} - 0.252 \times \text{Na}^+$, w/w) in polar ice core samples are used to identify volcanic signals in ice core records (Delmas et al., 1992; Cole-Dai et al., 1997, 2013). In the top 100.42 m of the DA2005 core, 78 volcanic signals are identified (Jiang et al., 2012) based on the nssSO_4^{2-} variation profile. For example, several large volcanic signals are found in the second half of the thirteenth century (Fig. 4b). The NO_3^- profile during this period shows several conspicuous dips at the times of the prominent volcanic signals marked by highly elevated nssSO_4^{2-} (Fig. 4b).

Reduced NO_3^- concentrations in ice layers containing high levels of

volcanic acid have been reported previously. For instance, R othlisberger et al. (2000, 2002) found in the Dome C, Antarctica and Greenland ice core records very low NO_3^- concentrations in ice layers with SO_4^{2-} peaks of volcanic origin and increased NO_3^- concentrations above and below these layers. It was proposed that the NO_3^- at the center of the volcanic ice layer is displaced by the volcanic acid into adjacent layers, resulting in reduced NO_3^- concentration in the volcanic layer and slightly elevated concentrations in the layers immediately above and below the volcanic layer (Wolff, 1995; R othlisberger et al., 2000, 2002).

The 78 volcanic signals in DA2005 are categorized, according to their normalized flux (volcanic flux normalized against that of the AD 1815 Tambora eruption), as those of large, moderate and small signals (Jiang et al., 2012). The displacement of NO_3^- is found in each of the 11 large signals (Fig. 4, one large signal was excluded due to suspected contamination). In addition, NO_3^- displacement occurs in 18 of the 24 moderate signals and 10 of the 42 small signals.

At the 11 large signals in the DA2005 core, the NO_3^- dips are significant, with the valley concentration in each dip $5.5\text{--}12.5 \mu\text{g kg}^{-1}$ lower than the local background concentration (30-year average concentration of NO_3^- before and after each volcanic signal), and the NO_3^- peak concentration on each shoulder is $2.6\text{--}14.2 \mu\text{g kg}^{-1}$ higher than its local background concentration (Fig. 4 and Table S1). However, the NO_3^- dips of the 10 small signals with displacement are rather minor, with the valley concentration in each dip $3.1\text{--}6.7 \mu\text{g kg}^{-1}$ lower than the local background, and NO_3^- concentrations on the shoulders are comparable to local background (Fig. 4b and d). It seems that the degree of NO_3^- displacement is largely dependent on the level of volcanic H_2SO_4 , and large volcanic signals will lead to significant displacement, while the small signals usually result in negligible displacement. These results support the proposed mechanism of NO_3^- displacement (Wolff, 1995; R othlisberger et al., 2002): high H_2SO_4 concentrations in an ice layer drive the equilibrium of $\text{H}^+ + \text{NO}_3^- \leftrightarrow \text{HNO}_3$ toward the right. The diffusion of the HNO_3 in the interstitial air of the snowpack transfers NO_3^- both up and down from the volcanic layer, resulting in a NO_3^- dip coincident with the SO_4^{2-} peak and slightly increased NO_3^- concentrations on the shoulders of the SO_4^{2-} peak. Consequently, high H_2SO_4 concentrations from large volcanic signals would favor HNO_3 formation and migration, leading to

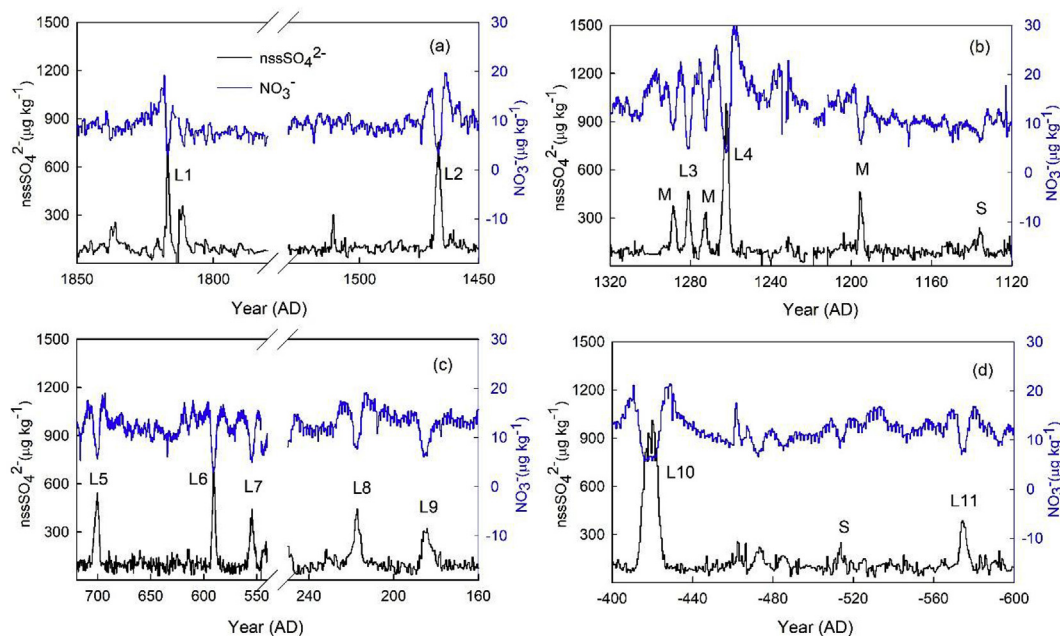


Fig. 4. Nitrate displacement in each of the 11 large volcanic signals (L1~L11) in the DA2005 core. Panel (b) shows the examples of volcanic signals of various magnitude on NO_3^- displacement, with L, M and S denoting large, moderate and small signals, respectively.

significant displacement of NO_3^- . The data in the DA2005 core indicate that the depletion of NO_3^- at the center of the volcanic nssSO_4^{2-} peak is exceedingly marked, i.e., the NO_3^- concentration decrease appears rather sharp. This is possibly the result of significant displacement aided by the long time of the volcanic peak in the snow/firn layers due to the extremely low accumulation rate at Dome A.

In the DA2005 core, the most recent NO_3^- displacement was found at the Tambora (1815) eruption located at 10.14 m depth (L1 in Fig. 4a). And no displacement is observed at volcanic signals after AD 1815 (i.e. AD 1816–1998), including the moderate signals of Krakatau (1883) and Agung (1963) eruptions. This pattern is generally similar to those in the Dome C ice record (Röthlisberger et al., 2002) and the South Pole ice record (Ferris et al., 2011), i.e., the most recent displacement occurring around AD 1815. However, in the top 114 m of the WDC06A core drilled at the WAIS Divide location (79.47°S, 112.08°W), no NO_3^- displacement was found at any eruption signals, even at large signal (e.g. Tambora at 1815). It is noted that the top 114 m of WDC06A core covering the last ~400 years has an average snow accumulation rate of about $200 \text{ kg m}^{-2} \text{ a}^{-1}$ (Cole-Dai et al., 2013). In the IND-22/B4 ice core covering the last ~450 years, located at DML (71.86°S, 11.54°E) with snow accumulation rate of $109 \text{ kg m}^{-2} \text{ a}^{-1}$, NO_3^- displacement by volcanic signals is not detected (Laluraj et al., 2011). Ca^{2+} is reported to be able to neutralize H_2SO_4 and prevent the formation of HNO_3 in case of high concentrations in Greenland ice core (Röthlisberger et al., 2002). However, Ca^{2+} concentrations in Antarctic ice cores are usually low. For example, average Ca^{2+} concentration in the WDC06A core is $1.6 \pm 1.2 \mu\text{g kg}^{-1}$, and no Ca^{2+} peaks are found in the period covered by the Tambora (1815) signal (Fig. S3) (Cole-Dai et al., 2013). Thus, no NO_3^- displacement occurring at Tambora in WDC06A core is unlikely caused by the effect of Ca^{2+} . Therefore, the difference between NO_3^- displacement in Dome A, Dome C and South Pole and no NO_3^- displacement in WAIS Divide and DML appears to be the result of different accumulation rates: significant NO_3^- displacement occurs only at locations of low accumulation rates in Antarctica; at sites with high snow accumulation ($> 100\text{--}200 \text{ kg m}^{-2} \text{ a}^{-1}$), no displacement of NO_3^- is observable in Antarctic ice records.

3. Conclusions

Examination of the data from the DA2005 core shows that the extremely low NO_3^- concentration results from a significant loss of snow NO_3^- due to a high degree of post-depositional processing, which is supported by the unusually high values of $\delta^{15}\text{N}$. The close relationships among the NO_3^- nitrogen and oxygen isotopes indicate that NO_3^- in the DA2005 core has undergone significant photolytic loss, and the preserved fraction in the core has gone through considerable cycling.

The low NO_3^- concentration during AD 1500–1900 in the DA2005 core is similar to the case detected in an ice core from DT263 (near Dome A), where it was suggested an unusually cold period in AD 1450–1850 occurred. Isotopes of DA2005 NO_3^- suggest that changes in NO_x sources are probably responsible for the low NO_3^- concentration during AD 1500–1900.

Volcanic SO_4^{2-} causes unusually notable NO_3^- displacement in the DA2005 core, in which the displacement is probably enhanced due to the extremely low accumulation rate. And the degree of displacement is largely determined by the volcanic signal magnitude, with large signals leading to substantial displacement, and small signals resulting in negligible displacement.

Acknowledgements

Financial support was provided by the National Natural Science Foundation of China (41476169, 40906098, 41576190) and Natural Science Foundation of Shanghai, China (14ZR1444000). Ice core analysis at South Dakota State University was supported in part by the US National Science Foundation (0839066). We thank the stable isotope

laboratory at University of Washington for providing technical support and assistance in analyzing the nitrate isotopic compositions in the DA2005 core. We thank all the members of the CHINARE 21 Inland Traverse (2004/05) for their contribution in collecting the ice core samples.

Appendix A. Supplementary data

Supplementary data to this article can be found online at <https://doi.org/10.1016/j.atmosenv.2019.06.031>.

References

- Alexander, B., Hastings, M.G., Allman, D.J., Dachs, J., Thornton, J.A., Kunasek, S.A., 2009. Quantifying atmospheric nitrate formation pathways based on a global model of the oxygen isotopic composition ($\Delta^{17}\text{O}$) of atmospheric nitrate. *Atmos. Chem. Phys.* 9, 5043–5056.
- Berhanu, T.A., Savarino, J., Erbland, J., Vicars, W.C., Preunkert, S., Martins, J.F., Johnson, M.S., 2015. Isotopic effects of nitrate photochemistry in snow: a field study at Dome C, Antarctica. *Atmos. Chem. Phys.* 15, 11243–11256.
- Blunier, T., Floch, G.L., Jacobi, H.-W., Quansah, E., 2005. Isotopic view on nitrate loss in Antarctic surface snow. *Geophys. Res. Lett.* 32, L13501.
- Cole-Dai, J., Ferris, D.G., Lanciki, A.L., Savarino, J., Thiemens, M.H., McConnell, J.R., 2013. Two likely stratospheric volcanic eruptions in the 1450s C.E. found in a bipolar, subannually dated 800 year ice core record. *J. Geophys. Res.* 118, 7459–7466.
- Cole-Dai, J., Mosley-Thompson, E., Thompson, L.G., 1997. Annually resolved southern hemisphere volcanic history from two Antarctic ice cores. *J. Geophys. Res.* 102, 16761–16771.
- Cole-Dai, J., Mosley-Thompson, E., Wight, S.P., Thompson, L.G., 2000. A 4100-year record of explosive volcanism from an East Antarctica ice core. *J. Geophys. Res.* 105, 24431–24441.
- Delmas, R.J., Kirchner, S., Palais, J.M., Petit, J.-R., 1992. 1000 years of explosive volcanism recorded at the South Pole. *Tellus B* 44, 335–350.
- Dibb, J.E., Talbot, R.W., Munger, J.W., Jacob, D.J., Fan, S.-M., 1998. Air-snow exchange of HNO_3 and NO_y at summit, Greenland. *J. Geophys. Res.* 103, 3475–3486.
- Elliott, E.M., Kendall, C., Wankel, S.D., Burns, D.A., Boyer, E.W., Harlin, K., Bain, D.J., Butler, T.J., 2007. Nitrogen isotopes as indicators of NO_x source contributions to atmospheric nitrate deposition across the midwestern and northeastern United States. *Environ. Sci. Technol.* 41, 7661–7667.
- EPICA Community Members, 2004. Eight glacial cycles from an Antarctic ice core. *Nature* 429, 623–628.
- Erbland, J., Savarino, J., Morin, S., France, J.L., Frey, M.M., King, M.D., 2015. Air-snow transfer of nitrate on the East Antarctic Plateau – Part 2: an isotopic model for the interpretation of deep ice-core records. *Atmos. Chem. Phys.* 15, 12079–12113.
- Erbland, J., Vicars, W.C., Savarino, J., Morin, S., Frey, M.M., Frosini, D., Vince, E., Martins, J.M.F., 2013. Air-snow transfer of nitrate on the East Antarctic Plateau – Part 1: isotopic evidence for a photolytically driven dynamic equilibrium in summer. *Atmos. Chem. Phys.* 13, 6403–6419.
- Ferris, D.G., Cole-Dai, J., Reyes, A.R., Budner, D.M., 2011. South Pole ice core record of explosive volcanic eruptions in the first and second millennia A.D. and evidence of a large eruption in the tropics around 535 A. D. *J. Geophys. Res.* 116, D17308.
- Fibiger, D.L., Hastings, M.G., 2016. First measurements of the nitrogen isotopic composition of NO_x from biomass burning. *Environ. Sci. Technol.* 50, 11569–11574.
- Fibiger, D.L., Hastings, M.G., Dibb, J.E., Huey, L.G., 2013. The preservation of atmospheric nitrate in snow at Summit, Greenland. *Geophys. Res. Lett.* 40, 3484–3489.
- France, J.L., King, M.D., Frey, M.M., Erbland, J., Picard, G., Preunkert, S., MacArthur, A., Savarino, J., 2011. Snow optical properties at Dome C (Concordia), Antarctica; implications for snow emissions and snow chemistry of reactive nitrogen. *Atmos. Chem. Phys.* 11, 9787–9801.
- Frey, M.M., Savarino, J., Morin, S., Erbland, J., Martins, J.M.F., 2009. Photolysis imprint in the nitrate stable isotope signal in snow and atmosphere of East Antarctica and implications for reactive nitrogen cycling. *Atmos. Chem. Phys.* 9, 8681–8696.
- Geng, L., Cole-Dai, J., Alexander, B., Erbland, J., Savarino, J., Schauer, A.J., Steig, E.J., Lin, P., Fu, Q., Zatzko, M.C., 2014. On the origin of the occasional spring nitrate peak in Greenland snow. *Atmos. Chem. Phys.* 14, 13361–13376.
- Grannas, A.M., Jones, A.E., Dibb, J., Ammann, M., Anastasio, C., Beine, H.J., Bergin, M., Bottenheim, J., Boxe, C.S., Carver, G., Chen, G., Crawford, J.H., Domine, F., Frey, M.M., Guzmán, M.I., Heard, D.E., Helmig, D., Hoffmann, M.R., Honrath, R.E., Huey, L.G., Hutterli, M., Jacobi, H.W., Klán, P., Lefler, B., McConnell, J., Plane, J., Sander, R., Savarino, J., Shepson, P.B., Simpson, W.R., Sodeau, J.R., von Glasow, R., Weller, R., Wolff, E.W., Zhu, T., 2007. An overview of snow photochemistry: evidence, mechanisms and impacts. *Atmos. Chem. Phys.* 7, 4329–4373.
- Hastings, M.G., Sigman, D.M., Lipschultz, F., 2003. Isotopic evidence for source changes of nitrate in rain at Bermuda. *J. Geophys. Res.* 108, 4790.
- Hastings, M.G., Sigman, D.M., Steig, E.J., 2005. Glacial/interglacial changes in the isotopes of nitrate from the Greenland Ice Sheet Project 2 (GISP2) ice core. *Glob. Biogeochem. Cycles* 19, GB4024.
- Hastings, M.G., Steig, E.J., Sigman, D.M., 2004. Seasonal variations in N and O isotopes of nitrate in snow at Summit, Greenland: implications for the study of nitrate in snow and ice cores. *J. Geophys. Res.* 109, D20306.
- Hoering, T., 1957. The isotopic composition of the ammonia and the nitrate ion in rain. *Geochem. Cosmochim. Acta* 12, 97–102.

- Isaksson, E., Karlén, W., Gundestrup, N., Mayewski, P., Whitlow, S., Twickler, M., 1996. A century of accumulation and temperature changes in Dronning Maud Land, Antarctica. *J. Geophys. Res.* 101, 7085–7094.
- Jacobi, H.-W., Hilker, B., 2007. A mechanism for the photochemical transformation of nitrate in snow. *J. Photochem. Photobiol.*, A 185, 371–382.
- Jiang, S., Cole-Dai, J., Li, Y., Ferris, D.G., Ma, H., An, C., Shi, G., Sun, B., 2012. A detailed 2840 year record of explosive volcanism in a shallow ice core from Dome A, East Antarctica. *J. Glaciol.* 58, 65–75.
- Jouzel, J., Masson-Delmotte, V., Cattani, O., Dreyfus, G., Falourd, S., Hoffmann, G., Minster, B., Nouet, J., Barnola, J.M., Chappellaz, J., Fischer, H., Gallet, J.C., Johnsen, S., Leuenberger, M., Loulergue, L., Luethi, D., Oerter, H., Parrenin, F., Raisbeck, G., Raynaud, D., Schilt, A., Schwander, J., Selmo, E., Souchez, R., Spahni, R., Stauffer, B., Steffensen, J.P., Stenni, B., Stocker, T.F., Tison, J.L., Werner, M., Wolff, E.W., 2007. Orbital and millennial Antarctic climate variability over the past 800,000 years. *Science* 317, 793–796.
- Kaiser, J., Hastings, M.G., Houlton, B.Z., Röckmann, T., Sigman, D.M., 2007. Triple oxygen isotope analysis of nitrate using the denitrifier method and thermal decomposition of N₂O. *Anal. Chem.* 79, 599–607.
- Lalraj, C.M., Thamban, M., Naik, S.S., Redkar, B.L., Chaturvedi, A., Ravindra, R., 2011. Nitrate records of a shallow ice core from East Antarctica: atmospheric processes, preservation and climatic implications. *Holocene* 21, 351–356.
- Lavigne, F., Degeai, J.-P., Komorowski, J.-C., Guillet, S., Robert, V., Lahitte, P., Oppenheimer, C., Stoffel, M., Vidal, C.M., Surono, Pratomo, I., Wassmer, P., Hajdas, I., Hadmoko, D.S., de Belizal, E., 2013. Source of the great A.D. 1257 mystery eruption unveiled, Samalas volcano, Rinjani Volcanic Complex, Indonesia. *Proc. Natl. Acad. Sci. U.S.A.* 110, 16742–16747.
- Legrand, M., Wolff, E., Wagenbach, D., 1999. Antarctic aerosol and snowfall chemistry: implications for deep Antarctic ice-core chemistry. *Ann. Glaciol.* 29, 66–72.
- Legrand, M.R., Kirchner, S., 1990. Origins and variations of nitrate in south polar precipitation. *J. Geophys. Res.* 95, 3493–3507.
- Li, Y., Cole-Dai, J., Zhou, L., 2009. Glaciochemical evidence in an East Antarctica ice core of a recent (AD 1450–1850) neoglaciation episode. *J. Geophys. Res.* 114, D08117.
- Ma, Y., Bian, L., Xiao, C., Allison, I., Zhou, X., 2010. Near surface climate of the traverse route from Zhongshan station to Dome A, East Antarctica. *Antarct. Sci.* 22, 443–459.
- Mayewski, P.A., Lyons, W.B., Zielinski, G., Twickler, M., Whitlow, S., Dibb, J., Grootes, P., Taylor, K., Whung, P.Y., Fosberry, L., Wake, C., Welch, K., 1995. An ice-core based, late Holocene history for the Transantarctic Mountains, Antarctica. *Contributions to Antarctic Research IV, Antarctic Research Series* 67, 33–45.
- Mayewski, P.A., Twickler, M.S., Whitlow, S.I., Meeker, L.D., Yang, Q., Thomas, J., Kreutz, K., Grootes, P.M., Morse, D.L., Steig, E.J., Waddington, E.D., Saltzman, E.S., Whung, P.-Y., Taylor, K.C., 1996. Climate change during the last deglaciation in Antarctica. *Science* 272, 1636–1638.
- McCabe, J.R., Boxe, C.S., Colussi, A.J., Hoffmann, M.R., Thiemens, M.H., 2005. Oxygen isotopic fractionation in the photochemistry of nitrate in water and ice. *J. Geophys. Res.* 110, D15310.
- McCabe, J.R., Thiemens, M.H., Savarino, J., 2007. A record of ozone variability in South Pole Antarctic snow: role of nitrate oxygen isotopes. *J. Geophys. Res.* 112, D12303.
- Michalski, G., Bhattacharya, S.K., Mase, D.F., 2012. Oxygen isotope dynamics of atmospheric nitrate and its precursor molecules. In: Baskaran, M. (Ed.), *Handbook of Environmental Isotope Geochemistry: Vol I*. Springer Berlin Heidelberg, Berlin, Heidelberg, pp. 613–635.
- Miller, D.J., Wojtal, P.K., Clark, S.C., Hastings, M.G., 2017. Vehicle NO_x emission plume isotopic signatures: spatial variability across the eastern United States. *J. Geophys. Res.* 122, 4698–4717.
- Mischler, J.A., Sowers, T.A., Alley, R.B., Battle, M., McConnell, J.R., Mitchell, L., Popp, T., Sofen, E., Spencer, M.K., 2009. Carbon and hydrogen isotopic composition of methane over the last 1000 years. *Glob. Biogeochem. Cycles* 23, GB4024.
- Pasteris, D., McConnell, J.R., Edwards, R., Isaksson, E., Albert, M.R., 2014. Acidity decline in Antarctic ice cores during the Little Ice Age linked to changes in atmospheric nitrate and sea salt concentrations. *J. Geophys. Res.* 119, 2013JD020377.
- Röthlisberger, R., Hutterli, M.A., Sommer, S., Wolff, E.W., Mulvaney, R., 2000. Factors controlling nitrate in ice cores: evidence from the Dome C deep ice core. *J. Geophys. Res.* 105, 20565–20572.
- Röthlisberger, R., Hutterli, M.A., Wolff, E.W., Mulvaney, R., Fischer, H., Bigler, M., Goto-Azuma, K., Hansson, M.E., Ruth, U., Siggaard-Andersen, M.-L., Steffensen, J.P., 2002. Nitrate in Greenland and Antarctic ice cores: a detailed description of post-depositional processes. *Ann. Glaciol.* 35, 209–216.
- Shi, G., Buffen, A.M., Hastings, M.G., Li, C., Ma, H., Li, Y., Sun, B., An, C., Jiang, S., 2015. Investigation of post-depositional processing of nitrate in East Antarctic snow: isotopic constraints on photolytic loss, re-oxidation, and source inputs. *Atmos. Chem. Phys.* 15, 9435–9453.
- Shi, G., Buffen, A.M., Ma, H., Hu, Z., Sun, B., Li, C., Yu, J., Ma, T., An, C., Jiang, S., Li, Y., Hastings, M.G., 2018a. Distinguishing summertime atmospheric production of nitrate across the East Antarctic ice sheet. *Geochem. Cosmochim. Acta* 231, 1–14.
- Shi, G., Hastings, M.G., Yu, J., Ma, T., Hu, Z., An, C., Li, C., Ma, H., Jiang, S., Li, Y., 2018b. Nitrate deposition and preservation in the snowpack along a traverse from coast to the ice sheet summit (Dome A) in East Antarctica. *Cryosphere* 12, 1177–1194.
- Sofen, E.D., Alexander, B., Steig, E.J., Thiemens, M.H., Kunasek, S.A., Amos, H.M., Schauer, A.J., Hastings, M.G., Bautista, J., Jackson, T.L., Vogel, L.E., McConnell, J.R., Pasteris, D.R., Saltzman, E.S., 2014. WAIS Divide ice core suggests sustained changes in the atmospheric formation pathways of sulfate and nitrate since the 19th century in the extratropical Southern Hemisphere. *Atmos. Chem. Phys.* 14, 5749–5769.
- Traversi, R., Becagli, S., Castellano, E., Cerri, O., Morganti, A., Severi, M., Udisti, R., 2009. Study of Dome C site (East Antarctica) variability by comparing chemical stratigraphies. *Microchem. J.* 92, 7–14.
- Vicars, W.C., Savarino, J., 2014. Quantitative constraints on the ¹⁷O-excess (Δ^{17} O) signature of surface ozone: Ambient measurements from 50°N to 50°S using the nitrate-coated filter technique. *Geochem. Cosmochim. Acta* 135, 270–287.
- Warren, S.G., Brandt, R.E., Grenfell, T.C., 2006. Visible and near-ultraviolet absorption spectrum of ice from transmission of solar radiation into snow. *Appl. Opt.* 45, 5320–5334.
- Watanabe, O., Kamiyama, K., Motoyama, H., Fujii, Y., Shoji, H., Satow, K., 1999. The paleoclimate record in the ice core at Dome Fuji station, East Antarctica. *Ann. Glaciol.* 29, 176–178.
- Weller, R., Traufetter, F., Fischer, H., Oerter, H., Piel, C., Miller, H., 2004. Postdepositional losses of methane sulfonate, nitrate, and chloride at the European project for ice coring in Antarctica deep-drilling site in Dronning Maud Land, Antarctica. *J. Geophys. Res.* 109, D07301.
- Wolff, E.W., 1995. *Nitrate in Polar Ice*. Springer Berlin Heidelberg, Berlin, Heidelberg, pp. 195–224.
- Wolff, E.W., Barbante, C., Becagli, S., Bigler, M., Boutron, C.F., Castellano, E., de Angelis, M., Federer, U., Fischer, H., Fundel, F., Hansson, M., Hutterli, M., Jonsell, U., Karlin, T., Kaufmann, P., Lambert, F., Littot, G.C., Mulvaney, R., Röthlisberger, R., Ruth, U., Severi, M., Siggaard-Andersen, M.L., Sime, L.C., Steffensen, J.P., Stocker, T.F., Traversi, R., Twarloh, B., Udisti, R., Wagenbach, D., Wegner, A., 2010. Changes in environment over the last 800,000 years from chemical analysis of the EPICA Dome C ice core. *Quat. Sci. Rev.* 29, 285–295.
- Wolff, E.W., Jones, A.E., Bauguutte, S.J.B., Salmon, R.A., 2008. The interpretation of spikes and trends in concentration of nitrate in polar ice cores, based on evidence from snow and atmospheric measurements. *Atmos. Chem. Phys.* 8, 5627–5634.
- Wolff, E.W., Jones, A.E., Martin, T.J., Grenfell, T.C., 2002. Modelling photochemical NO_x production and nitrate loss in the upper snowpack of Antarctica. *Geophys. Res. Lett.* 29, 5-1-5-4.
- Xiao, C., Li, Y., Hou, S., Ian, A., Bian, L., Ren, J., 2008. Preliminary evidence indicating Dome A (Antarctica) satisfying preconditions for drilling the oldest ice core. *Sci. Bull.* 53, 102–106.
- Xiao, H.Y., Liu, C.Q., 2002. Sources of nitrogen and sulfur in wet deposition at Guiyang, southwest China. *Atmos. Environ.* 36, 5121–5130.
- Yu, Z., Elliott, E.M., 2017. Novel method for nitrogen isotopic analysis of soil-emitted nitric oxide. *Environ. Sci. Technol.* 51, 6268–6278.
- Zatko, M., Geng, L., Alexander, B., Sofen, E., Klein, K., 2016. The impact of snow nitrate photolysis on boundary layer chemistry and the recycling and redistribution of reactive nitrogen across Antarctica and Greenland in a global chemical transport model. *Atmos. Chem. Phys.* 16, 2819–2842.
- Zatko, M.C., Grenfell, T.C., Alexander, B., Doherty, S.J., Thomas, J.L., Yang, X., 2013. The influence of snow grain size and impurities on the vertical profiles of actinic flux and associated NO_x emissions on the Antarctic and Greenland ice sheets. *Atmos. Chem. Phys.* 13, 3547–3567.
- Zielinski, G.A., Mayewski, P.A., Meeker, L.D., Whitlow, S., Twickler, M.S., Morrison, M., Meese, D.A., Gow, A.J., Alley, R.B., 1994. Record of volcanism since 7000 B.C. from the GISP2 Greenland ice core and implications for the volcano-climate system. *Science* 264, 948–952.